GEOPHYSICAL RESEARCH LETTERS, VOL. 32, L17108, doi:10.1029/2005GL023124, 2005

A first-principles model of spectrally resolved 5.3 μm nitric oxide emission from aurorally dosed nighttime high-altitude terrestrial thermosphere

J. W. Duff and H. Dothe
Spectral Sciences, Inc., Burlington, Massachusetts, USA

R. D. Sharma
Space Vehicles Directorate (VSBYB), Air Force Research Laboratory, Hanscom AFB, Massachusetts, USA

Received 4 April 2005; revised 21 July 2005; accepted 9 August 2005; published 13 September 2005.

[1] The spectrally resolved nighttime 5.3 μm emission from NO observed by the Cryogenic Infrared Radiance Instrumentation for Shuttle (CIRRIS-1A) experiment aboard space shuttle Discovery at 195 km tangent altitude during a strong auroral event is modeled using a first-principles kinetics model. An appropriate SHARC (Strategic High Altitude Radiance Code) Atmospheric Generator (SAG) is dosed with an IBC class III aurora. The spectrally resolved fundamental vibration-rotation band emissions from NO around 5.3 μm resulting from impacts of ambient NO with O as well as reactions of N atoms with O_2 are calculated under steady state conditions. The calculated results, using a local translational temperature derived from the observed spectrum, are in excellent agreement with the CIRRIS-1A observations, validating our model. The importance of the accurate nascent vibrational and rotational distribution of chemically produced NO as well as the collisonally induced rotation-to-vibration relaxation of rotationally hot NO is pointed out.

Citation: Duff, J. W., H. Dothe, and R. D. Sharma (2005), A first-principles model of spectrally resolved 5.3 μm nitric oxide emission from aurorally dosed nighttime high-altitude terrestrial thermosphere, *Geophys. Res. Lett.*, *32*, L17108, doi:10.1029/2005GL023124.

1. Introduction

[2] The 5.3 μm fundamental vibration-rotation band ($\Delta\nu = -1$; $\Delta j = 0, \pm 1$) emission from NO is the strongest cooling agent in the 110–300 km region of the terrestrial thermosphere [*Kockarts*, 1980; *Zachor et al.*, 1985; *Sharma et al.*, 1998; *Sharma and Roble*, 2001]. The 5.3 μm emission from the fundamental band as well as that from the overtone band ($\Delta\nu = -2$; $\Delta j = 0, \pm 1$) of NO around 2.7 μm are both greatly enhanced during an auroral event [*Sharma et al.*, 2000, 2001]. This is dramatically illustrated by the global images of 5.3 μm emission from NO taken by SABER (Sounding of the Atmosphere using Broadband Emission Radiometery) instrument aboard NASA's TIMED (Thermosphere-Ionosphere-Mesosphere Energetics and Dynamics) satellite on the 15 and 19 April 2002, before and after solar coronal mass ejection events, respectively [*Russell et al.*, 2002]. *Mlynczak et al.* [2003] point out that "the 5.3 μm limb radiance increases by a factor 5 to 7 during the storm time, and the altitude range over which the radiance is recorded increases by nearly 45 km," from 280 to 325 km tangent altitude. Since these emissions from NO are an important factor in determining the temperature and density structure of the atmosphere [*Sharma and Roble*, 2001], it is important that they be quantitatively modeled. In this letter we reexamine the model of the spectrally resolved emission from NO around 5.3 μm observed at 2293 LT on 29 April 1991 by the space shuttle experiment CIRRIS-1A for a tangent altitude of 195 km during a strong (IBC III) auroral event. In the previous effort to model this aurora [*Dothe et al.*, 2002] we were limited by the lack of knowledge of the temperature dependence of the rate coefficient of the $N(^2D) + O_2 \rightarrow NO + O$ reaction as well as the vibration-rotation distribution of the product NO. *Duff et al.* [2003] have since shown that this rate coefficient is given by the expression $k(T) = 6.2 \times 10^{-12}(T/300)$ cm^3/(s-molecule) instead of the nearly temperature independent value $2.8 \times 10^{-12}\exp(185/T)$ cm^3/(s-molecule) given in the literature [*Herron*, 1999]. *Sharma et al.* [2002] have in addition reported the vibrational-rotation distribution of the nascent NO produced by this reaction at room temperature.

[3] Figure 1 plots the calculated nighttime fundamental vibration-rotation NO band radiance (Watts/(cm^2-sr-cm^{-1})) as a function of frequency from a quiescent atmosphere at 195 km tangent altitude. The width of the P and R branches of the spectrum resulting from the inelastic impacts of ambient NO(v = 0) with O (blue curve) indicates low rotational temperature. The black curve is the chemiluminescent emission resulting from the nascent NO formed by the reaction $N(^4S) + O_2 \rightarrow NO + O$. This reaction is exothermic by 1.385 eV but has activation energy of about 0.3 eV [*Duff et al.*, 1994]. However, at the local translational temperature of 1065 K (0.092 eV) a significant fraction of atom-molecule pairs in the tail of the Maxwell-Boltzmann distribution have relative translational energy to overcome this barrier. Three R-branch bandheads, for $1 \rightarrow 0$, $2 \rightarrow 1$, and $3 \rightarrow 2$ vibrational transitions, are clearly identified and the fourth one for the $4 \rightarrow 3$ vibrational transition near 1920 cm^{-1} is apparent. Recalling that the rotational levels contributing to the bandheads have rotational energy in excess of 1 eV and noting the width of the emission envelope, one concludes that average rotational energy of the nascent NO produced by this reaction is at least several thousand degrees K. The emission due to

0094-8276/05/2005GL023124$05.00

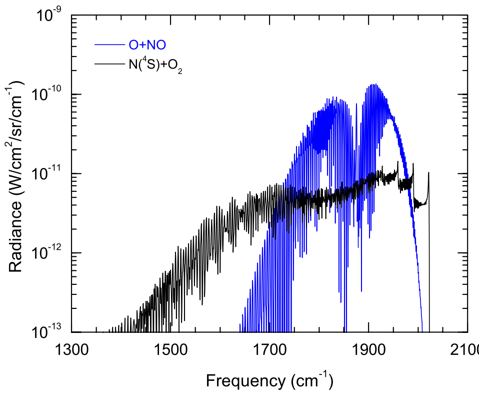

Figure 1. Contribution of the O + NO(v = 0) → NO(v′ = 1) + O vibrational excitation (blue curve) and the $N(^4S)$ + O_2 → NO(v) + O chemiluminescent reaction (black curve) to the ambient model spectrum.

$N(^2D)$ + O_2 → NO + O is not seen because of the absence of $N(^2D)$ atoms in the quiescent nighttime atmosphere, a conclusion supported by *Sharma et al.* [1996].

[4] Figure 2 plots the calculated nighttime fundamental vibration-rotation NO band radiance (Watts/(cm^2-sr-cm^{-1})) as a function of frequency from an IBC III aurorally dosed atmosphere at 195 km tangent altitude. Again, the blue curve is the emission resulting from the inelastic impacts, including pure rotational relaxation and vibrational rotational excitation, of ambient NO(v = 0, j) with O. The vibrational-rotational and pure rotational relaxation rate constants for O + NO(v, j) are based on quasi-classical trajectory calculations [*Duff et al.*, 1998] using information developed previously for O + NO(v) vibrational relaxation [*Duff and Sharma*, 1997]. The radiance level as well as the width of the P and R branches of the spectrum is larger than for the quiescent case (Figure 1) indicating a higher rotational temperature. This is because the reaction of $N(^4S)$ and $N(^2D)$ atoms with O_2 produce highly rotationally and vibrationally excited NO [*Duff et al.*, 1994; *Sharma et al.*, 2002] which, after losing the vibrational energy, is still highly rotationally excited. These highly rotationally excited NO molecules have a larger cross section for vibrational excitation upon impacts with O and yield vibrationally excited NO molecules with higher rotational temperature. The black curve is the chemiluminescent emission resulting from the nascent NO formed by the reaction $N(^4S)$ + O_2 → NO + O. The radiance level is enhanced over the quiescent case because of the production of $N(^4S)$ atoms by auroral dosing. The width of the emission spectrum is about the same as for the quiescent case indicating that energy going into the rotational degree of freedom is about the same. The red curve is the chemiluminescent emission resulting from the nascent NO formed by the reaction $N(^2D)$ + O_2 → NO + O. This reaction is exothermic by 3.76 eV, has no activation energy and produces NO in high rotational and vibrational levels. The rate coefficient of this reaction as function of rotational and vibrational quantum numbers of the nascent NO has been presented previously [*Duff et al.*, 2002; *Sharma et al.*, 2002]. The highly vibrationally and rotationally excited nascent NO molecules from the $N(^2D)$ + O_2 reaction lead, as shown by the red curve in Figure 2, to a few R-branch bandheads and emission over a large spectral range–a result of the calculated rotational temperature of the radiatively relaxed NO(v) produced by the $N(^2D)$ + O_2 reaction varying with the vibrational level v, 8400 K for v = 1 to 4400 K for v = 12.

[5] Figure 3 compares the CIRRIS-1A data and the sum of the curves of Figure 2 as well as the "standard model" [*Dothe et al.*, 2002]. Larger amounts of NO produced over the "standard model," because of the approximately three times faster $N(^2D)$ + O_2 rate coefficient of *Duff et al.* [2003] and thus a faster rate of excitation of rotationally hot NO(v = 0) by impacts with atomic oxygen, lead to a significant improvement in the agreement of the model with the CIRRIS-1A observations in the 1800–2000 cm^{-1} region of the spectrum. Furthermore, the detailed treatment (including vibrational-rotational excitation/de-excitation and radiative relaxation) of rotationally hot NO(v) from the $N(^2D)$ + O_2 reaction (average rotational temperature of ~5500 K) also leads to excellent agreement between the data and present model in the 1400–1700 cm^{-1} spectral region. The faster rate of excitation of rotationally hot

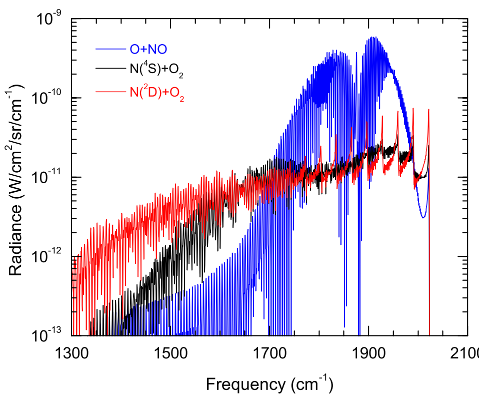

Figure 2. Contribution of the O + NO(v = 0) → NO(v′ = 1) + O vibrational excitation (blue curve), the $N(^4S)$ + O_2 → NO(v′, T_{rot}) + O (black curve) and $N(^2D)$ + O_2 → NO(v′, j′) + O (red curve) chemiluminescent reactions to the current model spectrum assuming an IBC III aurora.

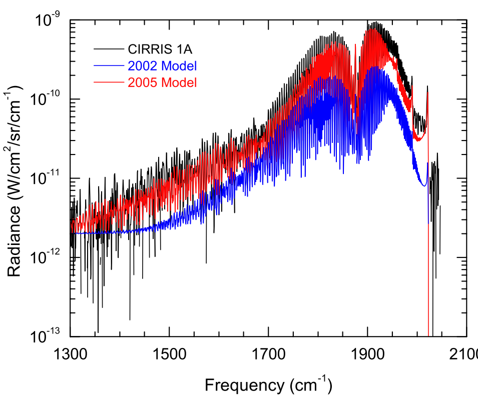

Figure 3. Calculated model spectrum (red curve) using the MSIS temperature of 1065 K and the observed auroral spectrum (black curve). Also shown is the "standard model" calculated spectrum (blue curve) [*Dothe et al.*, 2002].

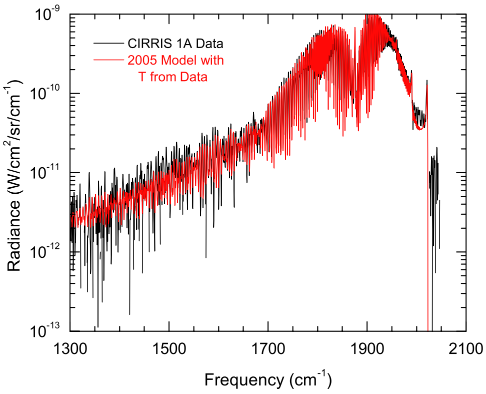

Figure 4. Calculated model spectrum (red curve) assuming a translational temperature of 1160 K derived from the CIRRIS-1A measurement and the observed auroral spectrum (black curve).

NO(v = 0) by impacts with atomic oxygen has implications for the remote sensing of NO by inversion of its 5.3 μm emission – an issue which is currently being investigated.

[6] The comparison shown in Figure 3 indicates that the model temperature (or spectral width) of the NO(v = 1) thermal emission in the 1800–2000 cm^{-1} spectral region is lower (or narrower) than that suggested by the observation. Our previous analysis [*Dothe et al.*, 2002] of the CIRRIS 1A spectrum indicated a rotational temperature of 925 ± 25 K for the thermal NO(v = 1 → v = 0) emission. Using the correlation between the temperature of the nascent NO(v = 1) rotational distribution and translational temperature developed previously [*Sharma and Duff*, 1997] implies a translational temperature approximately 25–30% higher than the rotational temperature. Extending our previous results shows that a NO(v′ = 1, j′) rotational distribution resulting from NO(v = 0, T) collisions with O in a thermal bath of T = 1160 K can be well represented by a Maxwell-Boltzmann distribution with a temperature of 925 ± 25 K. The derived translational temperature of 1160 ± 30 K at an altitude of 195 km is approximately 100 K greater than the MSIS temperature used in our previous and present models. Previous observations have also shown measured exospheric temperatures to be systematically higher than those predicted by MSIS during major geomagnetic storms [*Dymond et al.*, 2004].

[7] It should be noted that the data obtained by CIRRIS-1A is of high quality. Together with the earlier work [*Sharma et al.*, 1996, 1998] we estimate the signal-to-noise ratio in the observed spectra of 2.5–3 around 1400 cm^{-1}.

[8] Figure 4 compares the CIRRIS 1A observation with the present model using a translational temperature of 1160 K. The remaining discrepancy between the present model and CIRRIS 1A observation (Figure 3) in the 1800–2000 cm^{-1} spectral region is now removed, resulting in excellent agreement between the model and observation throughout the spectral range. This agreement requires a consistency between the atmospheric temperature, O + NO(v = 0, j) collisional excitation/de-excitation rate coefficients, and the rate coefficients for the NO vibrational-rotational distributions resulting from the reactions of $N(^4S)$ and $N(^2D)$ atoms with O_2.

[9] Figure 5 plots percent difference (=[(model x-model 1)/model 1]*100, x = 2, 3, and 4) between the current (model 1) with three other models. Model 2 and model 4 are the calculations using the MSISE-90 model atmosphere [*Hedin*, 1991] and NRLMSIS-00 [*Picone et al.*, 2002], respectively, together with the temperature independent $N(^2D) + O_2$ rate coefficient used recently by *Siskind et al.* [2004] to analyze rocket data. Model 2 differs from the "standard model" of *Dothe et al.* [2002] in that the latter uses the $N(^2D) + O_2$ rate coefficient recommended by *Herron* [1999]. Model 3 is the calculation using NRLMSIS together with the temperature dependent rate coefficient of *Duff et al.* [2003]. For Models 2 and 4, one would expect a decrease in radiance of a factor of about 4 around the band origin due to the decrease in the $N(^2D) + O_2$ chemiluminescence. However, the less than a factor of 4 decrease is due to the increased importance of the $N(^2D)$ + O quenching process compared to $N(^2D) + O_2$ reaction (which is now slower by a factor of about 4). This increases the amount of $N(^4S)$ and thus the importance of the $N(^4S) + O_2$ reaction. This is most important in the 1600–2000 cm^{-1} frequency range, where $N(^4S) + O_2$ reaction was previously of equal importance to (and is now of greater importance than) the $N(^2D) + O_2$ reaction. In the 1300–1600 cm^{-1} frequency range, the decrease in radiance is less due to the greater importance of the $N(^4S) + O_2$ reaction. It should be noted that the radiance calculated by models 2 and 4 differs uniformly by a factor roughly equal to the ratio of the O_2 density used in the two models. Model 3 differs uniformly from model 1 by a factor of about 2, again by a factor almost equal to the density ratio of O_2 used in the two models.

[10] The temperatures at an altitude of 195 km from both MSISE-90 (= 1065 K) and NRLMSISE-00 (= 1043 K) are both lower than the 1160 K temperature deduced from the CIRRIS-1A interferometer data. This affects mostly the NO fundamental emission due to the O+NO(v = 0) excitation mechanism, with a smaller effect around 1300–1700 cm^{-1}. Although the NRLMSISE-00 O_2 number density is a factor of 2.4 lower than MSISE-90, it is to be recalled that the strength of the aurora obtained from our analysis of the NO(Δv = 2) 2.7 μm radiometer data was based on the MSISE-90 atmosphere. If we used the lower O_2 density from NRLMSISE-00, then we would have estimated a

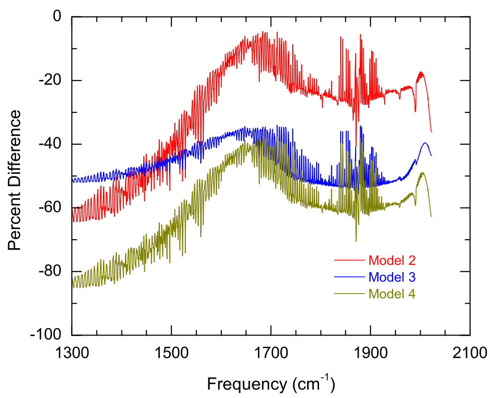

Figure 5. Percent difference (=[(model x-model 1)/model 1]*100, x = 2, 3, and 4) in the calculated radiances using different models as a function of frequency.

stronger aurora to compensate for the smaller production of NO.

[11] The earlier work of *Dothe et al.* [2002] showed that the 2002 model which assumes rotational LTE for NO produced by the $N(^2D) + O_2$ reaction, even after being multiplied by a factor of three underestimates the observed radiance around 1400 cm^{-1} by a factor of about 20. The current model using calculated high rotational temperatures gives excellent agreement with the radiance observed, not only in magnitude, but also in spectral shape. Since the vibrational transition probabilities in the first order are independent of the rotational quantum number, a change in the rotational temperature will just lead to increased in radiance in one part of the spectrum at the expense of another part. A quantitative assessment of the sensitivity of the observed spectrum to the rotational temperatures of different vibrational levels will be given in a later publication.

[12] In conclusion, the present model reproduces the CIRRIS-1A observation of strong nighttime aurora with a high degree of fidelity. It underscores the need to know both the rotational and vibrational distributions of the nascent NO produced by the chemiluminescent reactions to correctly model fundamental vibration-rotation band emission from NO during an auroral event.

[13] **Acknowledgment.** This research was in part funded by National Aeronautics and Space Administration research grant SRT03-0015 issued through the Office of Science Mission Directorate and Spectral Sciences, Inc. internal funds.

References

Dothe, H., J. W. Duff, R. D. Sharma, N. B. Wheeler, and J. O. Wise (2002), A model of odd nitrogen in the aurorally dosed nighttime terrestrial thermosphere, *J. Geophys. Res.*, *107*(A6), 1071, doi:10.1029/2001JA000143.

Duff, J. W., and R. D. Sharma (1997), Quasiclassical trajectory study of NO vibrational relaxation by collisions with atomic oxygen, *J. Chem. Soc., Faraday Trans.*, *93*, 2645–2649.

Duff, J. W., F. Bien, and D. Paulsen (1994), Classical dynamics of the $N(^4S) + O_2 \rightarrow NO(^2\Pi) + O(^3P)$ reaction, *Geophys. Res. Lett.*, *21*, 2043–2046.

Duff, J. W., H. Dothe, and R. D. Sharma (1998), Quasiclassical trajectory study of the rotational relaxation of vibrationally/rotationally excited NO by collisions with O atoms, *Eos Trans. AGU*, *79*(17), Spring Meet. Suppl., S304.

Duff, J. W., H. Dothe, and R. D. Sharma (2002), On the rate coefficient of the $N(^2D) + O_2$ reaction in the terrestrial thermosphere, *Eos Trans. AGU*, *83*(19), Spring Meet. Suppl., Abstract SA32A-06.

Duff, J. W., H. Dothe, and R. D. Sharma (2003), On the rate coefficient of the $N(^2D) + O_2 \rightarrow NO + O$ reaction in the terrestrial thermosphere, *Geophys. Res. Lett.*, *30*(5), 1259, doi:10.1029/2002GL016720.

Dymond, K. F., S. A. Budzien, S. E. Thonnard, A. C. Nicholas, R. P. McCoy, and G. Crowley (2004), Global observations of exospheric temperature during the Bastille Day event and comparisons with the TIMEGCM model and NRLMSIS-2000, *Eos Trans. AGU*, *85*(47), Fall Meet. Suppl., Abstract SA14A-03.

Hedin, A. E. (1991), Extension of the MSIS thermospheric model in the middle and lower atmosphere, *J Geophys. Res.*, *96*, 1159–1172.

Herron, J. T. (1999), Evaluated chemical kinetics data for reactions of $N(^2D)$, $N(^2P)$, and $N_2(A^3\Sigma_u^+)$ in the gas phase, *J. Phys. Chem. Ref. Data*, *28*, 1453–1483.

Kockarts, G. (1980), Nitric oxide cooling in the terrestrial thermosphere, *Geophys. Res. Lett.*, *7*, 137–140.

Mlynczak, M., et al. (2003), The natural thermostat of nitric oxide emission at 5.3 μm in the thermosphere observed during the solar storms of April 2002, *Geophys. Res. Lett.*, *30*(21), 2100, doi:10.1029/2003GL017693.

Picone, J. M., A. E. Hedin, D. P. Drob, and A. C. Aikin (2002), NRLMSISE-00 empirical model of the atmosphere: Statistical comparisons and scientific issues, *J. Geophys. Res.*, *107*(A12), 1468, doi:10.1029/2002JA009430.

Russell, J. M., et al. (2002), An overview and science results from the SABER experiment on TIMED satellite, *Eos Trans AGU*, *83*(47), Fall Meet. Suppl., SA61A-01.

Sharma, R. D., and J. W. Duff (1997), Determination of the translational temperature of the high altitude terrestrial thermosphere from the rotational distribution of the 5. 3 μm emission from NO(v = 1), *Geophys. Res. Lett.*, *19*, 2407–2410.

Sharma, R. D., and R. G. Roble (2001), Impact of the new rate coefficients for the vibrational deactivation of NO(v = 1) by O on the temperature and density structure of the terrestrial thermosphere, *J. Geophys. Res.*, *106*, 21,343–21,350.

Sharma, R. D., et al. (1996), Production of vibrationally and rotationally excited NO in the nighttime terrestrial thermosphere, *J. Geophys. Res.*, *101*, 19,707–19,713.

Sharma, R. D., H. Dothe, and J. W. Duff (1998), Model of the 5.3 μm radiance from NO during the daylit terrestrial thermosphere, *J. Geophys. Res.*, *103*, 14,753–14,768.

Sharma, R. D., N. B. Wheeler, J. O. Wise, H. Dothe, and J. W. Duff (2000), Global variation in the 2.7 μm NO overtone limb-emission from the lower thermosphere, *Geophys. Res. Lett.*, *27*, 349–352.

Sharma, R. D., R. O'Neil, H. Gardiner, J. Gibson, H. Dothe, J. W. Duff, P. P. Wintersteiner, and M. Kendra (2001), Midcourse Space Experiment: Auroral enhancement of nitric oxide medium-wave infrared emission observed by the Spatial Infrared Imaging Telescope III radiometer, *J. Geophys. Res.*, *106*, 21,351–21,365.

Sharma, R. D., H. Dothe, and J. W. Duff (2002), Mechanisms leading to NLTE IR emission in the terrestrial thermosphere and their impact on remote sensing of atmospheric parameters, *Proc. SPIE Int. Soc. Opt. Eng.*, *4882*, 117–121.

Siskind, D. E., J. M. Picone, M. H. Stevens, and K. Minschwaner (2004), Middle and upper thermospheric odd nitrogen: 1. A new analysis of rocket data, *J. Geophys. Res.*, *109*, A01303, doi:10.1029/2003JA009943.

Zachor, A., R. D. Sharma, R. M. Nadile, and A. T. Stair Jr. (1985), Inversion of a spectrally resolved limb radiance profile for the NO fundamental band, *J. Geophys. Res.*, *90*, 9776–9782.

H. Dothe and J. W. Duff, Spectral Sciences, Inc., 4 Fourth Ave., Burlington, MA 01803–5169, USA. (duff@spectral.com)

R. D. Sharma, Space Vehicles Directorate/VBYB, Air Force Research Laboratory, 29 Randolph Rd., Hanscom AFB, MA 01731-3010, USA. (ramesh.sharma@hanscom.af.mil)